Spatiotemporal Dynamics of Damped Propagation in Excitable Cardiac Tissue

Veniamin Y. Sidorov,[1] Rubin R. Aliev,[1] Marcella C. Woods,[2] Franz Baudenbacher,[1]
Petra Baudenbacher,[1] and John P. Wikswo[1,2,3]

[1]*Department of Physics and Astronomy, Vanderbilt University, Nashville, Tennessee 37235, USA*
[2]*Department of Biomedical Engineering, Vanderbilt University, Nashville, Tennessee 37235, USA*
[3]*Department of Molecular Physiology and Biophysics, Vanderbilt University, Nashville, Tennessee 37235, USA*

(Received 10 June 2002; revised manuscript received 29 August 2003; published 13 November 2003)

Compared to steadily propagating waves (SPW), damped waves (DW), another solution to the nonlinear wave equation, are seldom studied. In cardiac tissue after electrical stimulation in an SPW wake, we observe DW with diminished amplitude and velocity that either gradually decrease as the DW dies, or exhibit a sharp amplitude increase after a delay to become an SPW. The cardiac DW-SPW transition is a key link in understanding defibrillation and stimulation close to the refractory period, and is ideal for a general study of DW dynamics.

DOI: 10.1103/PhysRevLett.91.208104 PACS numbers: 87.19.Hh, 47.54.+r, 82.40.Ck, 89.75.Kd

Introduction.—The physics of the propagation of continuous waves in passive (linear) media has been studied exhaustively and exhibit reflection, refraction, and interference. In the classic example of electromagnetic (EM) waves in vacuum, waves of all frequencies propagate with the same phase velocity, so that a solitary EM pulse can propagate without distortion and can pass through another pulse unchanged. In lossy media, where energy is dissipated, wave amplitude decays as it propagates. In dispersive media, where wavelength depends upon propagation velocity, the wave shape can change with time and anomalous dispersion can occur.

In active (nonlinear) media, for which losses in the media are accompanied by the release of stored energy, solitary waves of a particular shape can propagate without distortion. The wave shape is determined by the governing nonlinear differential equations. Propagating nerve and cardiac action potentials (APs) are examples of solitary waves for which nonlinearities determine biologically important phenomena [1]: AP initiation requires a suprathreshold electrical stimulus, which in turn depends upon both the stimulus duration and the elapsed time since the previous AP. A minimum time interval, termed the absolute refractory period (ARP), must separate the leading edges of sequential APs, regardless of stimulus strength. Because of the ARP, upon collision APs will annihilate each other. Despite the common assumption that the AP has a constant shape and a uniform conduction velocity, experiments reveal that an AP following immediately after another AP will have a deformed shape (termed restitution) and reduced propagation velocity (termed dispersion) as compared to one after a longer separation in time [2]. Most of these phenomena are evident, for example, in reentrant cardiac arrhythmias [3]. Reduction of the threshold can increase the sensitivity to extraneous electrical activity and can lead to the spontaneous generation of waves that form expanding target patterns. AP annihilation upon collision results in a volume of tissue being refractory, so that any conduction through that region is blocked for a time longer than the ARP. Conduction block can lead to an AP that propagates over a closed path to form a vortex or more complex reentrant patterns [4]. A reduction in the ARP can lead to higher reentry frequencies, as seen in fibrillation, the most dangerous pattern of all cardiac reentries. Finally, there is an ongoing controversy as to whether reexcitation following an unsuccessful defibrillation shock arises from an unstable point focus (triggered activity), an intramural reentry not visible from the epicardium, or slow propagation in the electrically altered postshock tissue [5,6].

In this Letter, we demonstrate experimentally that nonuniform propagation and AP amplitude decay can play an important role in both conduction block and delayed activation. We used isolated rabbit hearts and applied a conditioning electrical stimulus (S_1), which produced a solitary AP propagating with constant shape and amplitude. Following a specified interval, we applied a second stimulus (S_2), which launches another wave into the wake of the initial one. This protocol is of special interest to the study of the vulnerability of the heart to the initiation of self-maintained, high frequency wave sources that have long been regarded as a precursor to dangerous cardiac arrhythmias [7–9]. A widely accepted mathematical description of vulnerability assumes that the effect of stimulation depends on the S_2 timing: an S_2 soon after S_1 dies out, because it is applied to absolutely refractory tissue; an S_2 long after S_1 freely propagates, because it is applied to resting tissue; an S_2 applied close to the boundary of absolute refractoriness may result in a discontinuous front that evolves into reentry (see Ref. [8] for details). This description bears its roots in the simple cellular automata model by Wiener and Rosenblueth [9], which assumes only discrete states of the medium occur; i.e., a wave either has a constant shape and propagates steadily, or it disappears. However, as mentioned above, theoretical and experimental observations indicate that the shape, amplitude, and velocity of a propagating wave are not always constant. Our experiments were designed to test quantitatively in cardiac tissue theoretical predictions regarding the spatiotemporal effects of S_2 stimulation in the wake of the previous conditioning wave, particularly those by Aliev and Panfilov in the Belousov-Zhabotinsky reaction [10].

Experimental procedures.—We used cryoablation to obtain a 1 mm thick, quasi-2D layer of left ventricular epicardium [11] from 2–3 kg New Zealand white rabbits ($n = 10$). We visualized the distribution of the transmembrane potential using a standard fluorescence mapping system, and we voltage calibrated the fluorescence images with microelectrode measurements [12]. We used the important pinwheel stimulation protocol [13]: to initiate planar conditioning S_1 waves propagating across the left ventricle, we placed a linear wire electrode, oriented perpendicular to the fibers, on the lower part of the left ventricular wall, and paced the heart at a cycle length of 300 ms. S_2 was applied with a point electrode approximately at the center of the imaging area. The current used for S_1 pacing was just above the threshold, whereas the current for the S_2 was 2 mA (about 20× diastolic threshold). The stimulus duration was 2 ms for S_1 and 10 ms for S_2 pulses. During each experiment, the S_1-S_2 interval was progressively shortened in 5–10 ms steps starting from 250 ms down to the ARP, when S_2 no longer produced a propagating wave. The slow-wave dynamics described below were observed in all ten hearts when S_2 was applied near the refractory tail of the S_1 response.

Results.—The results displayed in Figs. 1 and 2 depict the analysis for one typical recording using an S_1-S_2 interval of 180 ms and a 2 mA cathodal S_2. Figure 1 demonstrates the dynamics observed after application of S_2 close to the refractory period. The frames of the false color voltage movie in Fig. 1(a) show the response of the heart following S_2 termination. The movie starts at the end of S_2, which was applied when the preceding S_1 wave produced a gradient of repolarization in the vicinity of the S_2 electrode location. The S_1-induced planar wave had already propagated along the fiber direction from the lower right to the upper left of the image area, with the tail of the S_1 steadily propagating wave (SPW) disappearing in the upper-left corner of the 0 and 8 ms frames. As a result of S_2, two low-amplitude waves appear to propagate in opposite directions (arrows in the 16 ms frame). The wave moving left and upward dies out by 28 ms, while the wave propagating right and downward becomes a full amplitude response, which starts to propagate in all directions (last frame). A time lag of approximately 40 ms exists between the termination of S_2 and the appearance of the full amplitude response.

Figure 1(b) shows two damped waves (DW) forming following S_2 stimulation, which was applied to the refractory tail of the SPW from S_1, but only one DW causes a fully propagating wave front (S_2 SPW). More detailed spatiotemporal characteristics of the dynamics are illustrated in the time-space plot of Fig. 1(c), for which the data movie was sliced along the dashed α axis in panel (b). From this plot, one clearly sees that the left wave dies, while the wave on the right results in a full amplitude response.

Figures 2(a) and 2(b) show the DW dynamics in terms of signal upstroke (dV_m/dt). Figure 2(a) elucidates the wave front dynamics following S_2 stimulation (S_1 activity has been removed from the plot). The two waves propagate in opposite directions (white and black arrows) from the dog-bone shaped polarization [14] located at the center of the (x, y) plane. One of the waves decays, and the other transforms into a wave similar to the S_1-induced, high-amplitude SPW. Figure 2(b) demonstrates dV_m/dt amplitude for the two waves as a function of time along

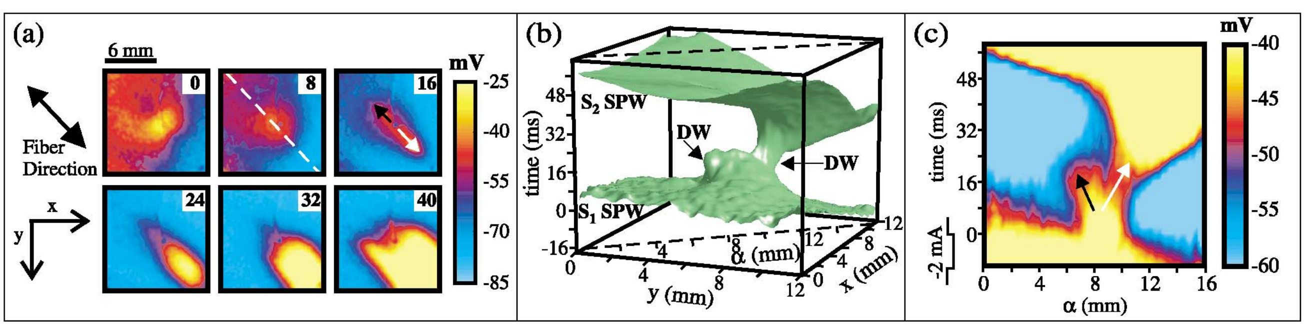

FIG. 1 (color). Damped propagation resulting from S_2 stimulation in the wake of a conditioning S_1 wave using a cathodal 2 mA, 10 ms S_2 (S_1-S_2 interval of 180 ms). (a) Frames of a movie of the transmembrane potential distribution, $V_m(x, y)$. The S_2 point electrode is located at the center of the images. The numbers in the upper right represent the time (ms) since S_2 termination. The arrows at 16 ms indicate DW propagation. (b) A 3D presentation of $V_m(x, y, t)$ following S_2 stimulation, constructed by stacking sequentially recorded 2D plots of $V_m(x, y)$, applying spatiotemporal filtering, and selecting $V_m = -50$ mV as the threshold to show the repolarization phase of the S_1 SPW and the post-S_2 activation dynamics. The dashed α axis is parallel to the fiber direction and corresponds to the white dashed line in the 8 ms image in panel (a). (c) The DW and S_2 SPW spatiotemporal dynamics. The time-space plot $V_m(\alpha, t)$ was constructed along the α axis. Black and white arrows indicate the propagation direction for the two DW. In all panels, S_2 ended at time = 0.

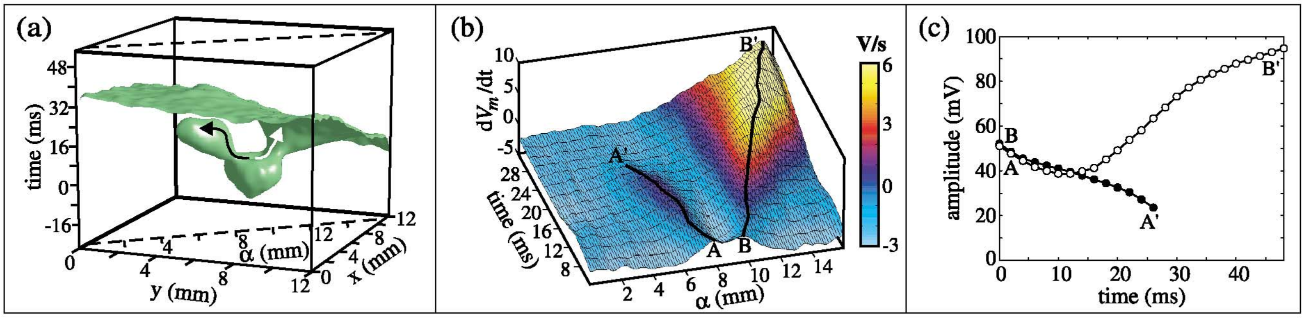

FIG. 2 (color). Detailed analysis of damped wave propagation. (a) 3D presentation of signal upstroke $[dV_m(x, y, t)/dt]$ following S_2 stimulation, constructed by stacking sequential 2D plots of $[dV_m(x, y, t)/dt]$, applying spatiotemporal filtering, and selecting $dV_m/dt = -1.1$ V/s as the threshold. The arrows indicate the DW with decaying propagation (black) and the growing wave (white). (b) $dV_m(\alpha, t)/dt$ as a function of time and space along the α axis. A-A' and B-B' are the two S_2 DW: A-A' decays and dies, while B-B' eventually grows into an SPW. (c) The amplitude of waves A-A' (filled circles) and B-B' (open circles) from (b). S_2 terminated at time = 0.

the dashed α axis in (a). The decaying wave, A-A', exhibits very small dV_m/dt until it finally dies, while for the other wave, B-B', dV_m/dt eventually increases. The crest position of the waves reflects the dynamics of the propagation velocity: A-A' has slower velocity (16.1 ± 0.5 cm/s) which approaches zero around 25 ms after S_2 termination, while B-B' exhibits a higher, fairly stable velocity for the interval shown (21.4 ± 0.4 cm/s). The two types of DW dynamics are clearly seen in Fig. 2(c). For A-A' the amplitude of the wave decreases with time until it disappears almost 25 ms after S_2 cessation (filled circles). B-B' (open circles) initially has similar dynamics, but instead of disappearing, eventually gains amplitude to produce a full-scale SPW.

The distance of low-amplitude DW propagation and the time delay between S_2 application and the transition of the DW into an SPW depends on the S_1-S_2 interval. Figure 3 illustrates the DW propagation distance and S_2-SPW delay as a function of the S_1-S_2 interval. The data presented in this figure were acquired from a different heart than the data shown in Figs. 1 and 2. Two phases are distinguishable in this curve: as the S_1-S_2 interval is decreased toward refractoriness, the character of the curve changes dramatically, with the distance and delay rising dramatically below 180 ms. This sharp change is caused by the transition of the stimulation mechanism from make to break [12,14]. In addition, the X-Z projection demonstrates approximately linear distance-delay dependence for S_1-S_2 intervals between 180 and 150 ms, indicating only a slight influence of the S_1-S_2 interval shortening on DW velocity (18.2 ± 2 cm/s). The minimal S_1-S_2 interval for response was 135 ms.

Discussion.—The "S_1-S_2" stimulation protocol has been widely used to study the cardiac response to premature stimulation. The dynamics are of special interest when the S_1-S_2 interval is close to the refractory period. We show damped propagating waves that either died out or evolved into a full-scale SPW. These dynamics are unusual from the point of view of classical theory [8] and, in our opinion, have received too little attention in either the theoretical or experimental literature.

Previously, the appearance of DW, sometimes referred to as decaying propagation, has been shown near the vulnerable window boundaries in both FitzHugh-Nagumo and Beeler-Reuter models of excitable media [8,15,16]. In a simulated nerve fiber using the 1D FitzHugh-Nagumo model under temperature gradient conditions, a slow-velocity, unstable wave and a fast-velocity, stable wave originating from the same point and traveling in opposite directions have also been demonstrated [17]. Recent findings show that multiple responses exist after a single stimulation near the boundary of a vulnerable window and are the result of propagation and conversion of DW into normal pulses [10]. Similar patterns were observed in a theoretical study of an inhomogeneous medium [18], where the patterns occurred near the boundary of an inhomogeneity. An interesting insight to the problem was recently suggested by Biktashev [19], who reformulated the classical Hodgkin-Huxley approach to excitable systems to include two equations describing the front of the pulse. He found that under proper conditions, propagation loses stability and becomes dissipative.

In experimental cardiac studies, responses different than all-or-none activity were initially reported by Kao and Hoffman [20]. They used isolated papillary muscles and Purkinje fibers to produce graded and decremental responses by varying the S_2 strength applied at a fixed time during repolarization or by varying the S_1-S_2 interval using a fixed S_2 strength. Additionally, the differences between the experimental study by Jalife and Moe, examining the role of passive tissue properties in conduction delay and impulse reflection [21], and the present work, describing an active response to stimulation in the repolarization phase, should be emphasized. They used an isotonic sucrose solution as an isolator to produce an unexcitable gap between the proximal and distal sections of a Purkinje strand preparation, such that the

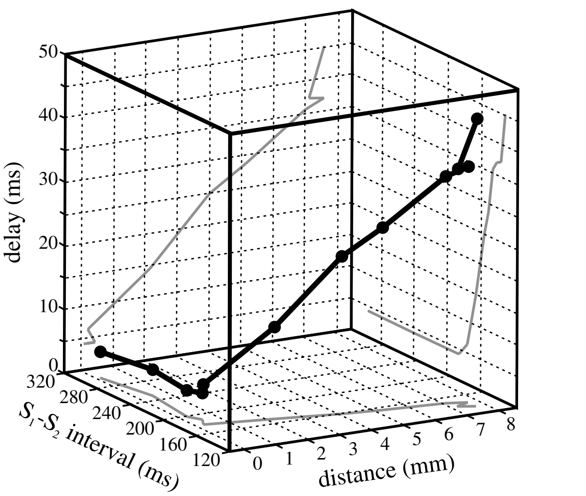

FIG. 3. The delay between S_2 and SPW appearance versus the distance between electrode position and location of SPW origination as a function of the S_1-S_2 interval. The threshold of 95 mV amplitude was used to locate the earliest conversion of DW to SPW. The delay was calculated as the period between S_2 onset and full amplitude response activation time $[(dV_m/dt)_{\max}]$. Projections of the curve onto the three axes are in gray. The sharp change in the curve corresponds to the transition of the stimulation mechanism from make to break.

transmission of the excitation between the two excitable segments is accomplished electrotonically by a passive response, in contrast to the active mechanism in our DW study.

It is important to note that, until now, DW dynamics have been experimentally studied only for chemical media in the Belousov-Zhabotinsky reaction [10]. Cardiac research has begun to address this subject in terms of a "graded response" [22]. Gotoh *et al.* [23] used a stimulation protocol similar to ours to investigate the induction of reentry and observed that a propagating lower-amplitude response could initiate normal activation distantly from the S_2 site. Although we suggest that the DW dynamics described in this present work may underlie the graded response effect, some important differences should be emphasized. Specifically, in contrast with this DW study in which S_2 monopolar cathodal pulses were applied in the wake of planar S_1 SPW, Gotoh *et al.* used bipolar electrodes for S_1 and S_2 stimulation, with the cathodal S_2 pole located nearer the S_1 and the S_2 poles oriented along the fiber direction. It has been shown that bipolar stimulation produces complex polarization patterns, which depends on both interelectrode distance and the position of the stimulating dipole with respect to the fiber direction [24]. Hence, the tissue response is determined not only by stimulus parameters but also by bipolar electrode location. Another important difference is the S_2 stimulus strength, in that Gotoh *et al.* studied vulnerability to reentry and hence examined high-amplitude stimulation. On the contrary, we used low intensity S_2 pulses to produce DW that could propagate over the polarization area.

Our work along with theoretical findings show that either functional inhomogeneity, which exists in the refractory tail [10], or an anatomical inhomogeneity [18] can result in damped propagation and, hence, demand a substantial revision of the classical explanation of vulnerability of cardiac tissue. Damped propagation must be examined in the context of apparent focal activity after a defibrillation shock [5]. We also conclude that cardiac tissue can serve as an ideal excitable medium to refine the measurement and understanding of the physics of damped propagation of waves in nonlinear, active media, particularly for reentrant, vortexlike excitation.

This work was supported by the NIH (R01-HL58241), by the AHA (0215128B), by gifts from William McMinn, and by the Academic Venture Capital Fund of Vanderbilt University.

[1] A. C. Scott, *Neurophysics* (John Wiley and Sons, New York, 1977), Chap. 4, pp. 90–104.
[2] J. M. Cao *et al.*, Circ. Res. **84**, 1318 (1999).
[3] *From Cell to Bedside*, edited by D. P. Zipes and J. Jalife (W. B. Saunders, Philadelphia, 2000), Chaps. 40–47, pp. 345–422.
[4] F. Fenton and A. Karma, Phys. Rev. Lett. **81**, 481 (1998).
[5] N. Chattipakorn *et al.*, J. Cardiovasc. Electrophysiol. **14**, 65 (2003).
[6] I. R. Efimov *et al.*, Circ. Res. **82**, 918 (1998).
[7] C. J. Wiggers and R. Wegria, Am. J. Physiol. **128**, 500 (1940).
[8] C. F. Starmer *et al.*, Biophys. J. **65**, 1775 (1993).
[9] N. Wiener and A. Rosenblueth, Arch. Inst. Cardiol. Mex. **16**, 205 (1946).
[10] R. R. Aliev and A. V. Panfilov, Phys. Rev. E **52**, 2287 (1995).
[11] M. A. Allessie *et al.*, Eur. Heart J. Suppl. E **10**, 2 (1989).
[12] V. Y. Sidorov, M. C. Woods, and J. P. Wikswo, Biophys. J. **84**, 3470 (2003).
[13] A. T. Winfree, *When Time Breaks Down* (Princeton University Press, Princeton, 1987), p. 128.
[14] J. P. Wikswo, S.-F. Lin, and R. A. Abbas, Biophys. J. **69**, 2195 (1995).
[15] K. Maginu, J. Math. Biol. **6**, 49 (1978).
[16] K. Maginu, J. Math. Biol. **10**, 133 (1980).
[17] R. Fitzhugh, *Biological Engineering* (McGraw-Hill, New York, 1969), pp. 1–85.
[18] G. B. Ermentrout and J. Rinzel, SIAM J Appl. Math. **56**, 1107 (1996).
[19] V. N. Biktashev, Phys. Rev. Lett. **89**, 168102 (2002).
[20] C. Y. Kao and B. F. Hoffman, Am. J. Physiol. **194**, 187 (1958).
[21] J. Jalife and G. K. Moe, Circ. Res. **49**, 233 (1981).
[22] N. A. Trayanova *et al.*, J. Cardiovasc. Electrophysiol. **14**, 756 (2003).
[23] M. Gotoh *et al.*, Circulation **95**, 2141 (1997).
[24] N. G. Sepulveda and J. P. Wikswo, J. Cardiovasc. Electrophysiol. **5**, 258 (1994).